Gut microbiota dysbiosis in stable coronary artery disease combined type 2 diabetes mellitus influence cardiovascular prognosis

Ran Tian
Peking Union Medical College Hospital
Honghong Liu
Peking Union Medical College Hospital
Siqin Feng
Peking Union Medical College Hospital
Haopeng Xu
Peking Union Medical College Hospital
Haiping Xing
Peking Union Medical College Hospital
Shuyang Zhang (shuyangzhang103@nrdrs.org)
Peking Union Medical College Hospital https://orcid.org/0000-0002-1532-0029

Original investigation

Keywords: Stable coronary artery disease, Type 2 diabetes mellitus, Metagenomics, Metabolomics, Multi-omics analysis, Cardiovascular prognosis

Posted Date: April 27th, 2020

DOI: https://doi.org/10.21203/rs.3.rs-23327/v1

Abstract

Background : Host-microbiota interactions involving metabolic pathways have been linked to the pathogenesis of cardiovascular diseases like atherosclerotic disease and diabetes. Since stable coronary artery disease patients combined with diabetes mellitus have significantly increased risk for cardiac event, we focused on elucidating the role of microbiota affecting cardiometabolic disease development.

Method : We used multi-omics analyses (metagenomics and metabolomics) of fecal and serum samples from a prospective cohort including stable coronary artery disease combined diabetes mellitus (SCAD+DM, n = 38), stable coronary artery disease (SCAD, n = 71), and healthy control (HC, n = 55). We connected microbiome features to disease severity in a three-pronged association analysis and identified prognostic bacterial biomarkers.

Results: We investigated bacterial and metabolic signatures of diabetic and atherosclerotic phenotypes. SCAD+DM individuals were characterized by increased levels of aromatic amino acids and carbohydrates, which correlate with a gut microbiome with enriched biosynthetic potential. Meanwhile, our study addressed how metformin may confound gut dysbiosis and increase the potential for nitrogen metabolism. What's more, we found that specific bacterial taxa Ruminococcus torques was predictive of cardiac survival outcomes.

Conclusions: Overall, our study identified relationships between features of the gut microbiota and circulating metabolites, providing a new direction for future studies aiming to understand the host–gut microbiota interplay in atherosclerotic cardiovascular pathogenesis.

Background

Reducing atherosclerotic cardiovascular disease (ASCVD) burden in diabetes mellitus is a major clinical imperative that should be prioritized to reduce premature death and the associated morbidity. Atherosclerotic cardiovascular disease remains the principal cause of death and disability among patients with type 2 diabetes mellitus (T2DM) [1, 2]. Key manifestations of ASCVD in diabetes mellitus include advanced clinical features, such as coronary heart disease, ischemic stroke, and peripheral artery disease. Studies have confirmed the importance of diabetes mellitus as an ASCVD risk factor in diverse populations and suggested T2DM as a risk equivalent for established coronary heart disease [3, 4]. T2DM is related to insulin resistance (IR) and islet β cell dysfunction, the clinical indicators, such as fasting blood glucose, glycated hemoglobin, and IR, are widely used in the diagnosis and classification of T2DM [5]. Cardiometabolic diseases, like diabetes and atherosclerosis, often results from interactions between genetic and environmental factors. It is estimated that genetic variation accounts for less than 10% of the overall metabolic phenotype. In addition, recent evidence suggests that environmental risks, including gut metagenome, is also responsible [6]. Finding pathogenic evidence for ASCVD-combined T2DM is of great importance, as this could assist in further understanding the pathogenesis of T2DM and provide a theoretical basis for its risk assessment, early diagnosis, and prevention strategies.

The human gut microbiome plays a major role in the production of vitamins, enzymes, and other compounds that digest and metabolize food, and regulate our immune system [7]. It can be considered as an endocrine organ, with remarkable dynamics and a major impact on our physiology. Several studies have reported gut microbiome dysbiosis as a factor in the rapid progression of insulin resistance in T2DM, which accounts for about 90% of all diabetes cases worldwide [8]. Gut microbiome dysbiosis may reshape intestinal barrier functions and host metabolic and signaling pathways, which are directly or indirectly related to insulin resistance. Thousands of the metabolites derived from microbes interact with the epithelial, hepatic, and cardiac cell receptors that modulate host physiology. Xenobiotics, including dietary components, antibiotics, and nonsteroidal anti-inflammatory drugs, strongly affect microbial composition of the gut and can promote dysbiosis. Any change in the gut microbiota can shift the host metabolism towards increased energy harvest during diabetes and atherosclerosis. However, the exact mechanisms behind the dynamics of gut microbes and their impact on host metabolism are yet to be deciphered.

We therefore performed a metagenome-wide association study of gut microbiome in SCAD-combined T2DM with a particular focus on the alterations of metabolic profiles. Using a multi-omics profiling approach, we identified specific features of the gut microbiota and host metabolites associated with insulin resistance and atherosclerosis and established relationships between several bacterial functional modules and serum metabotypes. We further showed the values of both taxa and metabolites in predicting cardiovascular outcomes prognosis. We also present evidence illustrating how metformin confounds the gut microbiome signature (an overview of the workflow is provided in Figure S1, Supporting information). Our study reveals the role of the gut microbiome in cardiometabolic disease pathogenesis, with potential implications for understanding host-microbiota interactions.

Methods

Cohort information

Study design and subjects: Study subjects were coronary artery disease patients who were hospitalized for coronary angiography in in Peking Union Medical College Hospital as previously described [9]. This study was approved by the Medical Ethics Committee of Peking Union Medical College Hospital (JS-1195). All subjects provided written informed consent. Subjects were further divided into three groups: (1) SCAD+DM, (2) SCAD, and (3) HC. The entry criteria were as follows: (1) SCAD+DM: subjects who were clinically diagnosed as SCAD and T2DM by cardiologists and endocrinologists. The diagnosis of SCAD was based on the presence of chest pain that did not change in pattern in the preceding two months with ≥50% stenosis in at least one main coronary [10]. (2) SCAD: subjects who were clinically diagnosed as SCAD without T2D history, and whose fasting blood glucose measured ≥ 7.0mmol/L or random blood glucose ≥ 11.1mmol/L during hospitalization were excluded. (3) HC: for controls, we enrolled healthy adolescents who exhibited negative results upon coronary computed tomography angiography (CCTA) or

coronary angiography examination or were identified as having no CAD-related clinical signs and symptoms. Inclusion and exclusion criteria were summarized as previously [9].

Phenotyping and metadata collection: Coronary atherosclerosis (AS) burden was estimated using the Gensini score, which was performed as previously reported [9]. HOMA-IR (Homeostatic model assessment of insulin resistance) was calculated as: (fasting plasma glucose (mmol/ l) × fasting serum insulin (mU/ l))/22.5 and HOMA-β (a measure of pancreatic beta-cell function) was calculated as (20 × fasting plasma insulin)/(fasting plasma glucose − 3.5) [11]. The collected metadata covered participants' anthropometric features and information related to health status, disease history, and medication use. Enzyme-linked immunosorbent assays (ELISAs) were conducted according to the manufacturer's instructions. The ELISA kits for IL-1β, TNF-α, IFN-γ, and high-sensitivity IL-6 were all purchased from R&D Systems, Inc. (Minneapolis, MN, USA) and used according to the manufacturer's instructions.

Follow-up study: Follow-up was conducted by telephone and medical chart abstraction to determine adverse outcomes. The primary endpoint was defined as a composite of all-cause death, nonfatal myocardial infarction, and nonfatal stroke. Main secondary endpoints were any coronary heart disease event including unstable angina, arrhythmia and congestive heart failure requiring hospitalization or an ischemia-driven coronary revascularization procedure such as invasive coronary angiography, percutaneous transluminal coronary intervention and coronary artery bypass graft. Medical records were accessed or requested to validate all self-reported events, which was defined using standard criteria, as described. The classification of events and follow-up data was made on the basis of phone interview and electronic medical records. Adjudication was conducted by 2 independent physicians who were blinded to the study.

Method for metagenomics

Stool sample collection and DNA extraction: Participants were given a stool sampler and provided detailed illustrated instructions for sample collection. Stool samples freshly collected from each participant were immediately transported to the laboratory and frozen at −80 °C. Fecal samples were thawed on ice and DNA extraction was performed using the Qiagen QIAamp DNA Stool Mini Kit (Qiagen) according to the manufacturer's instructions. DNA quantity was determined using a NanoDrop spectrophotometer, Qubit Fluorometer (with the Quant-iTTMdsDNA BR Assay Kit), and gel electrophoresis.

DNA library construction and sequencing of fecal samples: DNA library construction was performed following the manufacturer's instruction (Illumina). We used the same workflow as described previously to perform cluster generation, template hybridization, isothermal amplification, linearization, blocking and denaturation, and hybridization of the sequencing primers. We constructed one paired-end (PE) library with insert size of 350 bp for each sample, followed by high-throughput sequencing with PE reads of length 2 × 100 bp. High-quality reads were obtained by filtering low-quality reads with ambiguous "N"

bases, adapter contamination, and human DNA contamination from the Illumina raw reads, and by trimming low-quality terminal bases of reads simultaneously [12].

Metagenomic sequencing and gene catalogue construction: Employing the same parameters that were used to construct the MetaHIT gene catalogue [13], we performed gene prediction for the high quality reads using SOAPdenovo v1.06 [14] and GeneMark v2.7 [15], respectively. All predicted genes were aligned pairwise using BLAT and genes with over 90% of their length aligned to another with more than 95% identity (no gaps allowed) were removed as redundancies, resulting in a non-redundant gene catalogue. This gene catalogue from our Chinese samples was further combined with the previously constructed MetaHIT gene catalogue, by removing redundancies in the same manner.

Taxonomic annotation and abundance profiling: Taxonomic assignment of the predicted genes was performed using an in-house pipeline. In our analysis, we collected the reference microbial genomes from IMG database, and aligned genes onto the reference genomes. Based on the comprehensive parameter exploration of sequence similarity across phylogenetic ranks by MetaHIT enterotype paper [16], we used the 85% identity as the threshold for genus assignment, as well as another threshold of 80% for the alignment coverage. For each gene, the highest scoring hit(s) above these two thresholds was chosen for the genus assignment. For the taxonomic assignment at the phylum level, the 65% identity was used instead.

α-diversity and microbial community types (enterotypes): To estimate the genera richness of the sample, we calculated the within-sample (α)-diversity using the Shannon index based on genera profiles. A high α-diversity indicates a high richness of genera within the sample. The community types of each sample were analyzed by the PAM method using relative abundance of genera. The optimal number of clusters was estimated using the CH index, as previously described [16]. According to Spearman's correlation between genera abundances, the genera in enterotypes were clustered.

PCA and dbRDA: Principle component analysis (PCA) was performed on the genus level as previously described [17]. Distance-based redundancy analysis (dbRDA) was performed using Bray–Curtis distance, also on the genus level. dbRDA was used as a supervised complement to PCA, to better present the differences between ACVD and control samples. It is part of the vegan package of R 3.6.0.

KEGG analysis: Differentially enriched KO (Kyoto Encyclopedia of Genes and Genomes orthology) pathways or modules were identified according to their reporter score from the Z-scores of individual KOs (KEGG database release 59.0, genes from animals and plants removed). One-tail Wilcoxon rank-sum tests were performed on all KOs that occurred in more than five samples and adjusted for multiple testing using the Benjamin–Hochberg procedure. The Z-score for each KO could then be calculated. Absolute value of reporter score = 1.6 or higher (95% confidence on either tail, according to normal distribution) could be used as a detection threshold for significantly differentiating pathways.

Untargeted metabolomics study and serum metabolite data analysis

Sample analysis was performed on a Waters ACQUITY ultra-high-performance liquid chromatography system (Milford, MA, USA) coupled with a Waters Q-TOF Micromass system (Manchester, UK). The raw data were imported into Progenesis QI (Waters) for peak alignment to obtain a peak list containing the retention time, m/z, and peak area of each sample. The background and non-biologically relevant information were eliminated, and only variables with more than 80% of the nonzero measurement values were retained in the peak list [18, 19]. Open database sources, including the KEGG, MetaboAnalyst, Human Metabolome Database, and METLIN, were used to identify metabolic pathways. Next, the peak list was imported into SIMCA-P 14.0 software (Umetrics AB, Umea, Sweden) to acquire clustering information and important variables. To identify a biomarker for the pathophysiological development of the disease, metabolites with CV (coefficient of variation) values less than 30%, VIPs > 1, and adjusted *P*-values < 0.05 (Benjamini and Hochberg method, FDR) were selected as biomarker candidates for further statistical analysis. In this experiment, OPLS-DA analysis was used to identify the variables responsible for the discrimination.

Spearman multi-omics correlation analysis

Spearman correlations between functional modules, serum metabolites, and clinical parameters were calculated using R, and both differential abundances of IR- or AS-associated functional modules and metabolites were tested using the Wilcoxon rank sum test. Wherever mentioned, the Benjamini-Hochberg method was used to control the false discovery rate (FDR).

Feature selection using the random forest model

A random forest classifier was trained on 70% of the samples and tested on the remaining 30% of our samples using the random forest package in R. We used 10-fold cross-validation within the training set. Variable importance by mean decrease in accuracy was calculated for the random forest models. We built an optimal set of variables at the lowest cross-validation error. The predictive model was further applied for receiver operating characteristic (ROC) analysis. The area under the ROC curve (AUC) and confidence intervals for the ROC curves were calculated using the *pROC* R package.

Statistical analysis of metadata

Continuous variables were expressed as means with standard deviations in the case of normal distribution or medians with interquartile ranges when variables were not normally distributed. A Student's *t*-test or, where appropriate, a non-parametric Mann-Whitney U test was used to analyse differences between groups. Categorical data are expressed as numbers and percentages, and compared using the chi-squared test or Fisher's exact test. Kaplan-Meier curves were estimated for the survival distributions. The Log-rank test was used to test the difference in survival distributions between subgroups. Univariate Cox proportional hazard models were used to determine the effects of microbiota composition [20]. Hazard ratios and 95% confidence intervals were provided. All tests were two-sided. P values less than 0.05 were considered statistically significant. Statistical analysis was performed using IBM SPSS Statistics version 25 (IBM Inc., Armonk, NY, USA).

Results

Baseline Clinical Characteristics of Study Cohort

To explore the role of the microbiome composition in mediating clinical outcomes of SCAD+DM patients, we used a prospective cohort of coronary artery disease from PUMCH (Peking Union Medical College Hospital), China [9]. A total of 164 subjects were divided into the following groups based on guideline [21]: SCAD+DM group (N = 38), SCAD group (N = 71), and HC group (N = 55). The traditional cardiovascular risk factors of the 164 subjects are summarized in Table 1. There were significant differences in cardiovascular risk factors between the three study groups, except for triglyceride (TG) (P = 0.125), and high-sensitivity C-reactive protein (hs-CRP) (P = 0.113). Coronary atherosclerotic burden and severity were assessed using the Gensini score [22], indicating no significant difference between patients with or without T2DM (P = 0.298). We focused on the comparison of SCAD+DM versus SCAD. We observed a significant increase in body mass index (BMI) (P < 0.001), fasting blood glucose (FBG) (P < 0.001), and hemoglobin A1c (HbA1c) (P < 0.001) levels in the SCAD+DM group compared with the SCAD group. The medication usage rate of oral hypoglycemic agents (P < 0.001) and insulin (P < 0.001) were also significantly higher in the SCAD+DM group compared to the SCAD group. HOMA-IR [11] was used to assess insulin resistance, The SCAD+DM group showed a higher level than the SCAD group (P < 0.001). While HOMA-β, which reflected pancreatic β-cell function [11], was significantly lower in the SCAD+DM group compared to the SCAD group (P = 0.005). As for the expression of myocardial enzyme, there were significant differences between the two groups, such as creatine kinase (CK) (P = 0.028), creatine kinase-MB (CK-MB) (P = 0.015), and cardiac troponin-I (cTnI; P = 0.003). Although the results of cardiac catheterization did not reveal differences in the severity of atherosclerosis between SCAD+DM and SCAD groups, we suppose that glucose metabolism and myocardial damage were disturbed between the two groups.

Gut Microbial Diversity and Enterotype in SCAD and SCAD+DM

In order to investigate the gut microbiome of all study subjects, we performed metagenomic shotgun sequencing on a total of 164 fecal samples. After removing low-quality reads and human DNA reads, on average 58.6 million high-quality sequencing reads per sample were aligned to a comprehensive reference gut microbiome gene catalog comprising 9.9 million genes [23], which allowed, on average, 72.89 ± 2.42% of the reads in each sample to be mapped (Table S1), consistent with saturation of the gene-coding regions. The Shannon index and Simpson index were calculated to estimate the alpha diversity. The Shannon index at the genus level was much lower in SCAD and SCAD+DM groups (P = 0.04, HC vs. S; P = 0.005, HC vs. S+D; Wilcoxon rank sum test, Figure 1a). Consistently, the Simpson index was significantly decreased in both SCAD and SCAD+DM groups as compared to the controls (P = 0.016, HC vs. S; P = 0.006, HC vs. S+D; Wilcoxon rank sum test, Figure 1b). To assess the overall structure of the gut microbiota, the score plot of dbRDA (distance-based redundancy analysis) based on Bray-Curtis distances was constructed. The results indicated that the structure and composition of the microbiota differed significantly between different groups, even in SCAD vs. SCAD+DM comparison (P = 0.0017, H

vs. S; *P* = 0.0091, H vs. S+D; *P* = 0.0063, S vs. S+D; Permanova test, 9999 permutations; Figure 1c). The reduced richness of genera in the gut microbiota of SCAD-combined DM was consistent with previous findings [24], suggesting a possible deficiency of healthy microbiome in atherosclerotic cardiovascular disease.

Enterotypes were identified based on the abundance of genera, in order to explore the differences between microbial communities between different groups. The principal coordinate analysis (PCoA) using Jensen-Shannon distance was performed to cluster the 164 samples into two distinct enterotypes (Figure 1d). *Bacteroides* was the most enriched genus in enterotype 1, while *Prevotella* was the most enriched genus in enterotype 2 (*P* < 0.0001 and *P* < 0.0001, respectively; Wilcoxon rank sum test, Figure 1e). Both contributors in the two enterotypes have been reported in European and Chinese populations [12]. A higher percentage of HC and SCAD+DM patients were distributed in enterotype 1 (72.7% for HC, and 76.3% for S+D), while SCAD group showed a higher level of enterotype 2 (45.1% for S, Figure 1f). These findings suggest that enterotype 1 may represent bacterial structure associated with SCAD+DM, while enterotype 2 may be associated with SCAD.

SCAD and SCAD+DM Subjects Harbor Different Species of Gut Bacteria

To identify gut microbiota with potential value for SCAD and SCAD+DM diagnosis, we investigated bacterial alterations at the species level. The abundances of 13 bacterial species were observed to be significantly different in SCAD when compared with HC (Wilcoxon test *P* value < 0.05, absolute log2 fold change > 0.5). Six of these were SCAD-enriched while seven others were SCAD-depleted (Figure 2a, Table S2). Species were more abundant in the SCAD group, including *Fusobacterium ulcerans*, *Odoribacter splanchnicus*, and *Parabacteroides merdae*, while species like *Coprococcus eutactus*, *unclassified Ruminococcus sp. SR1/5*, and *unclassified Ruminococcus sp. 5_1_39BFAA* showed higher levels in the HC group. Compared to the HC group, the SCAD+DM subjects were characterized by 13 species, consisting of *Lactobacillus amylovorus*, *Veillonella parvula*, and *Parabacteroides distasonis*. Six species were decreased in the SCAD+DM group (relative to HCs) belonging to genera *Ruminococcus* and *Roseburia inulinivoran* (Figure 2b). Furthermore, in the SCAD vs. SCAD+DM comparison, 14 Species changed greatly (*P* < 0.05, Wilcoxon rank sum test), and five species were altered significantly (Absolute log2 fold change > 1). *Bifidobacterium longum*, *Bifidobacterium catenulatum*, and *Ruminococcus torques* were more abundant in patients with DM (*P* = 0.037, *P* = 0.025, *P* = 0.028, respectively, Wilcoxon test). While *Alistipes putredinis* and *Roseburia inulinivorans* were more abundant in the SCAD group (*P* = 0.029, *P* = 0.032, respectively, Wilcoxon test, Figure 2c). Recently, research identified that *Alistipes putredinis* was negatively correlated with OGTT (oral glucose tolerance test) response in gestational diabetes patients [25]. We further found that *Alistipes putredinis* was positively correlated with AS severity (*Rho*=0.3, *P*=0.0021), while negatively correlated with HbA1c% (*Rho*=-0.21, *P*=0.027) and HOMA-IR (*Rho*=-0.24, *P*=0.02). While *Bifidobacterium longum* was showed positively correlated with FBG levels (*Rho*=0.29, *P*=0.0038, Figure 2d).

The divergence of gut microbiota (GM) composition in each subject was assessed to explore the correlation of 171 species with 34 clinical indicators. We found that seven atherosclerotic phenotypes, including age, systolic blood pressure (SBP), New York Heart Association (NYHA) class, statin, total cholesterol (TC), TNF-α, and cTnI, were significantly associated with perturbated species abundance (Figure S2, Supporting information). Species belonging to the *Lactobacillus* genera were positively correlated to cTnI and tumor necrosis factor-α (TNF-α), while negatively correlated to TC. Species such as *Ruminococcus*, *Lachnospiraceae,* and *Streptococcus* were negatively associated with cTnI and positively associated with TC. In summary, we show that the microbiota composition differed between SCAD and SCAD+DM, and correlated with the major phenotype indicators of AS and DM.

Metabolic Profiling in SCAD and SCAD+DM Group

Considering the aberrant function profiles of gut microbes in disease subjects, we investigated the microbe-host interactions in atherosclerotic and diabetic metabolic diseases. As certain products of fermentation from the GM could enter the bloodstream and influence host physiology, we explored the host metabolic profile in fasting serum of a subset of 75 subjects using high-throughput liquid chromatography-mass spectrometry (LC/MS) and examined the relationship between GM and serum metabolites. Metabolomic profiling yielded 5461 features after eliminating impurity peaks and duplicate identifications. Based on the orthogonal projections to latent structures discriminant analysis (OPLS-DA) models of metabolite profiling data, we found that the serum metabolites were significantly separated between all SCAD patients with or without DM and healthy controls. The compositional changes in patients involved 66 analytes that were significantly different between HC vs. SCAD, and 118 analytes between HC vs. SCAD+DM (detailed in Methods Section). There were 15 metabolites, which were obviously different, in both SCAD and SCAD+DM groups as compared to the control (Figure 3a). Notably, these metabolites exhibited statistically analogous profiles of alterations in SCAD and SCAD+DM, which agreed with our gut microbiome findings (Table S3).

We identified a collection of differentially produced compounds belonging to both host-derived and bacterial-derived metabolites. Sixty metabolites of this collection were found significantly associated with glycometabolic indicators, including FBG, HbA1c, HOMA-IR, HOMA-β, and atherosclerosis associated factors, such as number of stenosed vessels and cTnI levels (Figure 3b, Table S4). These metabolites were separated into groups that were either positively or negatively correlated with insulin resistance (hereafter represented by IR+ or IR-, respectively) or atherosclerosis severity (AS+ or AS-, respectively). Among these, IR+ metabotypes including carboxylic acid, glucuronic acid, benzoic acid, and amino acids, were positively correlated with FBG, HbA1c, and HOMA-IR levels, while negatively correlated with HOMA-β. Surprisingly, these IR+ metabotypes were even associated with the severity of atherosclerosis. While other metabolites, such as leucine, glutarylglycine, and terpene lactone, were negatively correlated with insulin resistance and AS severity. Moreover, the IR+ and AS+ metabotypes were positively correlated metformin and other oral antidiabetic drugs, while negatively associated with interleukin1β (IL-1β) levels, which is a classic proinflammatory cytokine linked to atherosclerosis [(26)]. AS+ metabotypes were found to be positively correlated to traditional risk factors, such as SBP, smoke, hyperlipidemia, IL-6, TNF-α. The IR-

and AS- metabotypes were generally negatively related to these phenotypes (Figure S3). Taken together, these results suggested that the SCAD+DM patients had significantly different metabolite profiles compared with SCAD, and closely related to diabetes and atherosclerotic indicators.

Functional alteration in GM Linked to Metabolic Metabotypes of SCAD and SCAD+DM

Using the Kyoto Encyclopedia of Genes and Genomes (KEGG) [27] database, we evaluated gut microbial functions across groups in our study cohort. All genes were aligned to the KEGG database and assigned to the KEGG orthology (KO), after cross-comparison, we identified 356 KO in total (Table S5, Supporting information). Principal component analysis (PCA), based on KO, revealed striking differences in microbial functions at the first principal component (PC1) between HC and SCAD ($P < 0.0001$, Wilcoxon rank sum test) and SCAD vs. SCAD+DM ($P < 0.001$, Wilcoxon rank sum test, Figure S4a, Supporting information). Thereafter, we investigated the metabolic potential of the gut microbiome in relation to these metabolites using KEGG functional modules consisting of KOs (Figure S1e, Supporting information). The KOs collection set were clustered into 67 microbiome functional modules, and 21 of the 67 microbiome functional modules were significantly associated (Wilcoxon rank sum test, FDR < 0.05) with one or more of the IR and AS phenotypes. All 21 functional modules were furthermore associated with the IR and AS associated metabotypes (Figure 4), with a majority also differing in abundance in the expected direction in the cohort (Figure S4b, Supporting information). By abundance comparison, we found that the AS- metabotypes, consisting of L-leucine and cyclic alcohol derivatives, were generally highly abundant in healthy subjects. While AS+ metabotypes were more abundant in SCAD and SCAD+DM groups (Figure 3c).

The cross-domain associations between the IR and AS phenotypes, the serum metabolome, and the gut microbiome described above may suggest functional relationships. Notably, the functional modules that were negatively associated with AS + metabotypes involved carbohydrate metabolism, including nucleotide sugar biosynthesis, galactose degradation, amino sugar metabolism, two-component system, and bacterial secretion systems. In contrast, the microbial functional modules positively associated with AS + metabotypes contained fatty acid synthesis pathways and aromatic amino acid metabolism. In addition, microbial modules positively correlated with IR, primarily including the metabolism of cysteine and methionine, cofactors and vitamins, and amino sugar and nucleotide sugar systems. Study have showed that some of these microbial pathways have elevated expression in gut microbiomes when transplanted into mice from obese donors [28].

Microbial and Metabolites Features Predict Major Adverse Cardiac Event

After identifying differences in intestinal microbial composition between SCAD and SCAD+DM in our cohort, we examined whether microbial and metabolic signature would enable prediction of major adverse cardiac event (MACE) based on baseline status of the cohort. Recent study showed that connection of longitudinal profiling of glucose metabolism with multi-omics profiling facilitating the precision medicine goal of defining diseases on the basis of molecular mechanisms and

pathophysiology [29]. The definitions of primary and secondary outcomes were detailed summarized in Method. During a median follow-up period of 18.6 months (interquartile range: 18–22.7 months), we effectively followed up 109 patients totally. No significant difference was found in the endpoint event comparison between the two groups (Table 2). We built a classification model based on random forest using the explanatory variables of species, metabolites and KEGG modules to exploit the prediction efficacy of MACE outcomes with a tenfold cross-validation. The model performance was evaluated with an area under the curve (AUC) of receiver operating characteristic (ROC). Using the initial relative abundance of differentially abundant species or metabolites solely, the performance was the lowest (AUC = 0.63, 95% CI 0.43-0.81; AUC=0.6, 95% CI 0.35-0.82, respectively) (Figure 5a). The prediction performance was significantly improved by using the metabolites combined with KEGG modules (AUC = 0.70, 95% CI 0.44-0.91). However, the model incorporating data on both species and metabolites showed the best performance (AUC = 0.71, 95% CI 0.4-0.83), indicating the power of shotgun metagenomics for predicting host phenotypes. The features with predictive value were metabolites including carboxylic acid, norfuraneol, 3b-Hydroxy-5-cholenoic acid while species containing *Ruminococcus torques*, *Edwardsiella ictaluri-tarda* and *Bifidobacterium longum* (Figure 5b).

We then stratified subjects into high versus low categories based on their median relative abundance of these features selected. Significantly better outcomes were predicted for MACE with higher abundance of *Bifidobacterium.longum* (Hazard Ratio [HR] = 2.652, 95% confidence interval [CI] 1.17–4.92), *Ruminococcus.torques* (HR = 2.363, 95% CI 1.08–4.56), and 3,8-Dihydroxy-1-methylanthraquinone-2-carboxylic acid (HR = 4.53, 95% CI 1.43–11.79) (Figure 5c). The high accuracy of our prediction models indicates that the initial condition of the gut microbiota could be a potential predictive tool for cardiovascular prognosis outcomes. Furthermore, the performance comparisons of our models suggest that combining the features of both microbiome and metabolomics improves the prediction accuracy.

Metformin Alters Gut Microbiome Signatures in SCAD+DM Patients

Metformin is the most prescribed pharmacotherapy for individuals with type 2 diabetes, accumulating evidence indicates that microbial changes might contribute to the antidiabetic effect of metformin [30]. We further divided the SCAD+DM population into two subgroups, namely metformin treated (Metformin+, n=18) and metformin untreated (Metformin-, n = 20). Multivariate analysis showed significant (PERMANOVA = 0.045) differences in gut taxonomic composition between metformin untreated and metformin treated groups, consistent with a broad-range of dysbiosis in T2DM (Figure 6a). To further interpret the therapeutic effects of metformin on gut microbiota shifts, we observed that gene richness significantly increased in the T2DM metformin+ microbiome, but was reduced in T2DM metformin- microbiomes (P = 0.0186, Wilcoxon rank sum test, Figure 6b). We then compared T2D metformin+ and T2D metformin- subjects to characterize the treatment effect in more detail. Univariate tests of the effects of metformin treatment showed a significant increase of *unclassified Clostridum spp.* and a reduced abundance of *Prevotella bryantii.*, *Citrobacter koseri*, and *Acidaminococcus fermentans* (Figure 6c).

We further explored gut microbiome alterations in metformin-untreated compared with metformin-treated subjects using univariate tests of microbial taxonomic and functional differences, with significant trends shown in Figure 6d. *Citrobacter koseri* was more abundant in Metformin- subgroup while *Escherichia coli* and *Shewanella frigidimarina* exhibited high levels in the Metformin+ subgroup. Functionally, we found enrichment of pyrimidine metabolism and modules for nitrogen metabolism varied significantly. *Citrobacter koseri* exhibited a strong negative correlation with nitrification and complete nitrification, implicating the interaction of metformin with gut bacteria.

Discussion

In the current study, we determined that both SCAD and SCAD+DM patients presented with significantly different metabolite profiles and gut microbiota compared to healthy controls, and further shift between SCAD combined with T2DM or without. By integrating data on host phenotypes, gut microbiome, and fasting serum metabolome, we were able to demonstrate clear metabolome signatures of IR and AS associated phenotypes. Both on a compositional and functional level, we found significant microbiome alterations that are consistent with side effects of metformin treatment. What's more, our study suggests that microorganisms may affect cardiometabolic disease pathogenesis and specific bacterial genus was predictive of cardiac survival outcomes.

Microbiota diversity is essential to maintain ecosystem stability and efficiency. We found that the microbial composition of cardiometabolic disease was associated with lower α-diversity compared to HCs. Generally speaking, a high α-diversity is considered evidence of a "good" health status [(31)]. Our data revealed that bacterial communities in diabetic patients with SCAD presented with lower taxa richness than those in the non-diabetic group. Reduction in gut microbial diversity breaches the cell-to-cell integrity, which causes a leaky gut with enhanced permeability that leads to intestinal inflammation and reduced or disturbed immune response at the gut mucosa [(32)]. In order to clearly explore the compositional variation of the gut microbiome in individuals with cardiovascular and diabetic complications, we conducted species-level analysis. We found that species belonging to *Ruminococcus genera*, *Coprococcus eutactus*, *Enterobacter hormaechei/cloacae*, and *Streptococcus thermophilus* were more enriched in the HC group. *Ruminococcus* are important in maintaining intestinal homeostasis and are involved in the conversion of host-ingested dietary polysaccharides into host-usable nutrients [(33)] and it was proven to be associated with numerous health benefits, such as reducing risk of diabetes [(34)]. And the primary health benefit of *Streptococcus thermophilus* is the ability to improve gastrointestinal tract function [(35)]. When compared with the HC group, SCAD combined with T2DM owned higher levels of *Parabacteroides distasoni*, which was further positively correlated with traditional cardiovascular risk factors. A previous Taiwanese study showed that the presence of *Parabacteroides distasonis* was positively associated with obesity [(36)]. Surprisingly, we found an increased abundance of probiotics in SCAD+DM patients. Among them, seven species belong to *Lactobacillus* genera and two species belong to *Bifidobacterium* genera. *Lactobacillus helveticus*, *Lactobacillus gasseri,* and *Lactobacillus johnsonii* were positively correlated with atherosclerosis markers, including cTnI, total cholesterol, and TNF-α levels.

Although many animal researches have strengthened that *Bifidobacterium* play protective role in T2D, while *Bifidobacterium* has not been used alone as probiotics for T2D in human [37, 38]. In addition, the evidence of probiotics is limited as conflicting results were revealed in certain trials where probiotics did not exert any effect on glycaemic parameters [39, 40]. In summary, our data suggested that the composition of the gut microbiome in SCAD individuals changes when combined with diabetes.

The human gut microbiota interacts extensively with the host through metabolic exchange and substrate co-metabolism. Metabolic phenotypes revealed significant differences between SCAD patients and SCAD+DM patients in the current study, suggesting that cardiometabolic disease may involve a universal metabolic disturbance. Similar to our previous findings, AS negatively related metabolic modules are typically abundant in healthy subjects, while AS positively associated metabotypes are more concentrated in the disease group [9]. IR- metabotypes include metabolites, such as leucine, glutarylglycine, and terpene lactone. Studies have confirmed that branched chain amino acids (BCAAs) including leucine are significantly associated with IR in both obese and T2DM subjects [41, 42]. However, several studies have pointed out that BCAA levels are reduced in diabetic patients [43, 44]. We speculate that the inconformity of metabolomics may be due to drug effects or inconsistent inclusion criteria. Terpene lactones are produced as a result of standardized preparations of Ginkgo biloba leaf extract which retain certain bioactive characteristics, making it an attractive add-on therapeutic for patients with ischemic cardiovascular and cerebrovascular diseases [45]. Several animal studies have reported on the antidiabetic activity of lactones [46]. However, we did not observe the main classes of gut microorganism-dependent metabolites that have been linked to CVD risk, such as TMAO, perhaps owing to differences between Chinese and Western diets. Overall, through inter-group comparisons and correlation analysis with clinical indicators, we identified metabotypes exhibited significant alterations between SCAD patients combined T2DM.

By integrating multi-omics data, we were able to demonstrate potential microbial pathway signatures of AS or IR phenotypes. Both metabolome and microbial functional analysis indicated essential potential for carbohydrate metabolism and aromatic amino acid metabolism in AS development. Glucose is the primary source of human energy, and research shows that T2DM patients exhibit increased glycolysis [47, 48]. Other study has also revealed an expansion of the gut microbiome toward enzymatic degradation of plant-derived carbohydrates [49]. Consistent relationships in our data between serum concentrations of carboxylic acids, bacterial carbohydrates biosynthesis, and the severity of IR phenotypes are reinforced by the intriguing findings that carbohydrates pathway co-vary with fasting serum metabolites. Meanwhile, as indicated by the results, our metabolic profile showed that aromatic compounds, such as benzoic acid, which are normally generated and biosynthesized by bacterial species, significantly perturbed the development of atherosclerosis [50]. Phenolic and indolic compounds are typical products of bacterial metabolism of aromatic amino acids, while dietary phenolic compounds are often transformed prior to absorption [51]. Positive correlations between microbial functions (aromatic amino acids biosynthesis) and AS positive associated metabotypes, suggest that they may impact host

metabolism to some extent. Therefore, we conclude that dysbiosis of the human gut microbiota impacts the serum metabolome and contributes to cardiometabolic disease.

In particular, we observed significant changes in Escherichia abundance across all sampling points in the metformin-treated group, a finding that is in agreement with results reported in a cross-sectional study that compared metformin treatment with T2DM. The effects of metformin on the abundance of Escherichia spp. are likely indirect, and possibly, a result of modified bacteria–bacteria interactions or due to other physiological and/or environmental changes within the gut upon metformin treatment [30]. Functional analyses showed that gut microbiota of metformin-treated T2DM patients exhibited increased potential for nitrogen metabolism, which was consistent with previous findings reporting that metformin modulates nitrogen and urea metabolism [52]. Further, increased nitrogen catabolism commonly associated with diabetes, was rebalanced upon metformin treatment [53]. In conclusion, our results suggest partial gut microbial mediation of both therapeutic and adverse effects induced by the most widely used antidiabetic medication, metformin, although further validation is required to conclude causality and to clarify how such mediation might occur.

Mounting evidence in this metagenomic era provides new insights into the role of microbiota in the pathogenesis and prognosis of CVD [54, 55]. Importantly, we found that the combination signature of bacterial taxa and metabolite may represent a promising prognosis biomarker for cardiac event. Presence of *Ruminococcus torques*, one of the top features enriched in SCAD+DM, was highly predictive of long-term survival in the cardiometabolic cohort. Research have found that the abundance of *Ruminococcus torques* decreased after bariatric surgery and diabetes remission which may further implicate the effect of *Ruminococcus torques* on diabetes [56]. In the future, omics approach sequencing could be used to stratify patients for cardiovascular risk, including microbiome interventions. More physiological studies are needed to elucidate how the intestinal carbohydrates and other amino acids enter the bloodstream and from which intestinal location they are absorbed. Furthermore, investigations of how dietary changes, alone or in combination with microbial or pharmacological interventions, may impact the microbiome and how modulation of serum metabolite levels will present novel avenues to counter the pathogenesis of IR and its linked epidemics of common metabolic and cardiovascular disorders.

Conclusions

Type 2 diabetes mellitus is a highly prevalent metabolic disorder characterized by an imbalance in blood glucose levels and insulin resistance. T2DM confers an increased risk of CVD, most stable coronary artery disease patients with T2DM fall into a high CVD risk category. Therefore, the identification of an effective and convenient biomarker for monitoring lipid and glucose metabolism disorder is very important for prevention of major cardiac events. Mounting evidence shows that key members of the gut microbiome play a role in the rapid progression of insulin resistance, but most studies on gut microbial variations lacked consideration for the risk presented when CAD combined with T2DM. Our results showed that alterations in the gut microbial community and serum metabolites in SCAD+DM, and alterations in the

gut microbiota, were correlated with AS and IR phenotypes via the mediation of serum metabolites. Furthermore, altered gut microbiota mediates some of metformin's antidiabetic effects by influencing certain pathways. These findings may provide new insights for revealing novel potential aetiology for AS, understanding the role of gut microbiota in cardiometabolic diseases, and modulating gut microbiota as a therapeutic target.

Abbreviations

ASCVD: atherosclerotic cardiovascular disease

SCAD: Stable coronary artery disease

T2DM: Type 2 diabetes mellitus

HC: Healthy control

CVD: Cardiovascular disease

AS: Atherosclerosis

MACE: Major adverse cardiac event

GM: Gut microbiota

IR: Insulin resistance

CCTA: Coronary computed tomography angiography

HOMA-IR: Homeostatic model assessment of insulin resistance

HOMA-β: Homeostatic model assessment of beta-cell function

PCA: Principle component analysis

PcoA: Principal coordinate analysis

dbRDA: Distance-based redundancy analysis

OPLS-DA: Orthogonal projections to latent structures discriminant analysis

KO: Kyoto Encyclopedia of Genes and Genomes orthology

ROC: Receiver operating characteristic

AUC: Area under the ROC curve

TG: Triglyceride

hs-CRP: High-sensitivity C-reactive protein

BMI: Body mass index

FBG: Fasting blood glucose

TC: Total cholesterol

LDL-C: Low-density lipoprotein cholesterol

HDL-C: High-density lipoprotein cholesterol

HbA1c: Hemoglobin A1c

CK: Creatine kinase

CK-MB: Creatine kinase-MB

cTnI: Cardiac troponin-I

SBP: Systolic blood pressure

NYHA-class: New York Heart Association class

TNF-α: Tumor necrosis factor-α

IL-1β: Interleukin1β

HR: Hazard Ratio

CI: Confidence interval

FDR: False discovery rate

BCAA: Branched chain amino acid

Declarations

Ethics approval and consent to participate

The study was approved by local ethics committees (Peking Union Medical College Hospital, Beijing) and informed consent was obtained from all subjects (JS-1195).

Consent for publication

Not applicable.

Availability of data and materials

Not applicable.

Competing interests

The authors declare no competing interests.

Funding

This work was supported by National Natural Science Foundation of China (81670329), CAMS Innovation Fund for Medical Sciences (CIFMS) (No. 2016-I2M-1-011).

Authors' contributions

R. Tian and SY. Zhang designed and coordinated the study. HH. Liu and SQ. Feng were in charge of patient recruitment and sample collection. HP. Xu and HP. Xing participated in follow up visit. HH. Liu and SQ. Feng carried out the bioinformatic analyses of metagenomic and metabolomics data. R. Tian and HH. Liu wrote the manuscript. SY. Zhang revised the manuscript. All authors read and approved the final manuscript.

Acknowledgements

We thank Si Tang for sample collection and Lifeng Liang for technical assistance.

References

1. Paneni F, Beckman JA, Creager MA, Cosentino F. Diabetes and vascular disease: pathophysiology, clinical consequences, and medical therapy: part I. European heart journal. 2013;34(31):2436-43.
2. Low Wang CC, Hess CN, Hiatt WR, Goldfine AB. Clinical Update: Cardiovascular Disease in Diabetes Mellitus: Atherosclerotic Cardiovascular Disease and Heart Failure in Type 2 Diabetes Mellitus - Mechanisms, Management, and Clinical Considerations. Circulation. 2016;133(24):2459-502.
3. Bulugahapitiya U, Siyambalapitiya S, Sithole J, Idris I. Is diabetes a coronary risk equivalent? Systematic review and meta-analysis. Diabetic medicine : a journal of the British Diabetic Association. 2009;26(2):142-8.
4. Howard BV, Best LG, Galloway JM, Howard WJ, Jones K, Lee ET, et al. Coronary heart disease risk equivalence in diabetes depends on concomitant risk factors. Diabetes care. 2006;29(2):391-7.
5. Roden M. [Diabetes mellitus: definition, classification and diagnosis]. Wiener klinische Wochenschrift. 2016;128 Suppl 2:S37-40.
6. Burcelin R, Serino M, Chabo C, Blasco-Baque V, Amar J. Gut microbiota and diabetes: from pathogenesis to therapeutic perspective. Acta diabetologica. 2011;48(4):257-73.

7. Tremaroli V, Backhed F. Functional interactions between the gut microbiota and host metabolism. Nature. 2012;489(7415):242-9.
8. Pedersen HK, Gudmundsdottir V, Nielsen HB, Hyotylainen T, Nielsen T, Jensen BA, et al. Human gut microbes impact host serum metabolome and insulin sensitivity. Nature. 2016;535(7612):376-81.
9. Liu H, Chen X, Hu X, Niu H, Tian R, Wang H, et al. Alterations in the gut microbiome and metabolism with coronary artery disease severity. Microbiome. 2019;7(1):68.
10. Montalescot G, Sechtem U, Achenbach S, Andreotti F, Arden C, Budaj A, et al. 2013 ESC guidelines on the management of stable coronary artery disease: the Task Force on the management of stable coronary artery disease of the European Society of Cardiology. European heart journal. 2013;34(38):2949-3003.
11. Matthews DR, Hosker JP, Rudenski AS, Naylor BA, Treacher DF, Turner RC. Homeostasis model assessment: insulin resistance and beta-cell function from fasting plasma glucose and insulin concentrations in man. Diabetologia. 1985;28(7):412-9.
12. Qin J, Li Y, Cai Z, Li S, Zhu J, Zhang F, et al. A metagenome-wide association study of gut microbiota in type 2 diabetes. Nature. 2012;490(7418):55-60.
13. Qin J, Li R, Raes J, Arumugam M, Burgdorf KS, Manichanh C, et al. A human gut microbial gene catalogue established by metagenomic sequencing. Nature. 2010;464(7285):59-65.
14. Li R, Zhu H, Ruan J, Qian W, Fang X, Shi Z, et al. De novo assembly of human genomes with massively parallel short read sequencing. Genome research. 2010;20(2):265-72.
15. Zhu W, Lomsadze A, Borodovsky M. Ab initio gene identification in metagenomic sequences. Nucleic acids research. 2010;38(12):e132.
16. Arumugam M, Raes J, Pelletier E, Le Paslier D, Yamada T, Mende DR, et al. Enterotypes of the human gut microbiome. Nature. 2011;473(7346):174-80.
17. Li J, Zhao F, Wang Y, Chen J, Tao J, Tian G, et al. Gut microbiota dysbiosis contributes to the development of hypertension. Microbiome. 2017;5(1):14.
18. Cheng ML, Wang CH, Shiao MS, Liu MH, Huang YY, Huang CY, et al. Metabolic disturbances identified in plasma are associated with outcomes in patients with heart failure: diagnostic and prognostic value of metabolomics. Journal of the American College of Cardiology. 2015;65(15):1509-20.
19. Li Y, Song X, Zhao X, Zou L, Xu G. Serum metabolic profiling study of lung cancer using ultra high performance liquid chromatography/quadrupole time-of-flight mass spectrometry. Journal of chromatography B, Analytical technologies in the biomedical and life sciences. 2014;966:147-53.
20. Heller G. The Cox proportional hazards model with a partly linear relative risk function. Lifetime data analysis. 2001;7(3):255-77.
21. 10. Cardiovascular Disease and Risk Management: Standards of Medical Care in Diabetes-2019. Diabetes care. 2019;42(Suppl 1):S103-s23.
22. Gensini GG. A more meaningful scoring system for determining the severity of coronary heart disease. The American journal of cardiology. 1983;51(3):606.

23. Li J, Jia H, Cai X, Zhong H, Feng Q, Sunagawa S, et al. An integrated catalog of reference genes in the human gut microbiome. Nature biotechnology. 2014;32(8):834-41.
24. Sanchez-Alcoholado L, Castellano-Castillo D, Jordan-Martinez L, Moreno-Indias I, Cardila-Cruz P, Elena D, et al. Role of Gut Microbiota on Cardio-Metabolic Parameters and Immunity in Coronary Artery Disease Patients with and without Type-2 Diabetes Mellitus. Frontiers in microbiology. 2017;8:1936.
25. Wu Y, Bible PW, Long S, Ming WK, Ding W, Long Y, et al. Metagenomic analysis reveals gestational diabetes mellitus-related microbial regulators of glucose tolerance. Acta diabetologica. 2019.
26. Libby P. Interleukin-1 Beta as a Target for Atherosclerosis Therapy: Biological Basis of CANTOS and Beyond. Journal of the American College of Cardiology. 2017;70(18):2278-89.
27. Kanehisa M, Araki M, Goto S, Hattori M, Hirakawa M, Itoh M, et al. KEGG for linking genomes to life and the environment. Nucleic acids research. 2008;36(Database issue):D480-4.
28. Ridaura VK, Faith JJ, Rey FE, Cheng J, Duncan AE, Kau AL, et al. Gut microbiota from twins discordant for obesity modulate metabolism in mice. Science (New York, NY). 2013;341(6150):1241214.
29. Schussler-Fiorenza Rose SM, Contrepois K, Moneghetti KJ, Zhou W, Mishra T, Mataraso S, et al. A longitudinal big data approach for precision health. Nature medicine. 2019;25(5):792-804.
30. Wu H, Esteve E, Tremaroli V, Khan MT, Caesar R, Manneras-Holm L, et al. Metformin alters the gut microbiome of individuals with treatment-naive type 2 diabetes, contributing to the therapeutic effects of the drug. Nature medicine. 2017;23(7):850-8.
31. Structure, function and diversity of the healthy human microbiome. Nature. 2012;486(7402):207-14.
32. Paun A, Yau C, Danska JS. The Influence of the Microbiome on Type 1 Diabetes. Journal of immunology (Baltimore, Md : 1950). 2017;198(2):590-5.
33. La Reau AJ, Meier-Kolthoff JP, Suen G. Sequence-based analysis of the genus Ruminococcus resolves its phylogeny and reveals strong host association. Microbial genomics. 2016;2(12):e000099.
34. Lagier JC, Million M, Hugon P, Armougom F, Raoult D. Human gut microbiota: repertoire and variations. Frontiers in cellular and infection microbiology. 2012;2:136.
35. Doron S, Snydman DR. Risk and safety of probiotics. Clinical infectious diseases : an official publication of the Infectious Diseases Society of America. 2015;60 Suppl 2:S129-34.
36. Chiu CM, Huang WC, Weng SL, Tseng HC, Liang C, Wang WC, et al. Systematic analysis of the association between gut flora and obesity through high-throughput sequencing and bioinformatics approaches. BioMed research international. 2014;2014:906168.
37. Gurung M, Li Z, You H, Rodrigues R, Jump DB, Morgun A, et al. Role of gut microbiota in type 2 diabetes pathophysiology. EBioMedicine. 2020;51:102590.
38. Sasaki M, Ogasawara N, Funaki Y, Mizuno M, Iida A, Goto C, et al. Transglucosidase improves the gut microbiota profile of type 2 diabetes mellitus patients: a randomized double-blind, placebo-controlled

study. BMC gastroenterology. 2013;13:81.

39. Andreasen AS, Larsen N, Pedersen-Skovsgaard T, Berg RM, Moller K, Svendsen KD, et al. Effects of Lactobacillus acidophilus NCFM on insulin sensitivity and the systemic inflammatory response in human subjects. The British journal of nutrition. 2010;104(12):1831-8.
40. Mazloom Z, Yousefinejad A, Dabbaghmanesh MH. Effect of probiotics on lipid profile, glycemic control, insulin action, oxidative stress, and inflammatory markers in patients with type 2 diabetes: a clinical trial. Iranian journal of medical sciences. 2013;38(1):38-43.
41. Menni C, Fauman E, Erte I, Perry JR, Kastenmuller G, Shin SY, et al. Biomarkers for type 2 diabetes and impaired fasting glucose using a nontargeted metabolomics approach. Diabetes. 2013;62(12):4270-6.
42. Huffman KM, Shah SH, Stevens RD, Bain JR, Muehlbauer M, Slentz CA, et al. Relationships between circulating metabolic intermediates and insulin action in overweight to obese, inactive men and women. Diabetes care. 2009;32(9):1678-83.
43. Salek RM, Maguire ML, Bentley E, Rubtsov DV, Hough T, Cheeseman M, et al. A metabolomic comparison of urinary changes in type 2 diabetes in mouse, rat, and human. Physiological genomics. 2007;29(2):99-108.
44. Zhang X, Wang Y, Hao F, Zhou X, Han X, Tang H, et al. Human serum metabonomic analysis reveals progression axes for glucose intolerance and insulin resistance statuses. Journal of proteome research. 2009;8(11):5188-95.
45. Liu XW, Yang JL, Niu W, Jia WW, Olaleye OE, Wen Q, et al. Human pharmacokinetics of ginkgo terpene lactones and impact of carboxylation in blood on their platelet-activating factor antagonistic activity. Acta pharmacologica Sinica. 2018;39(12):1935-46.
46. Silva EAP, Carvalho JS, Guimaraes AG, Barreto RSS, Santos MRV, Barreto AS, et al. The use of terpenes and derivatives as a new perspective for cardiovascular disease treatment: a patent review (2008-2018). Expert opinion on therapeutic patents. 2019;29(1):43-53.
47. Lu J, Zhou J, Bao Y, Chen T, Zhang Y, Zhao A, et al. Serum metabolic signatures of fulminant type 1 diabetes. Journal of proteome research. 2012;11(9):4705-11.
48. Messana I, Forni F, Ferrari F, Rossi C, Giardina B, Zuppi C. Proton nuclear magnetic resonance spectral profiles of urine in type II diabetic patients. Clinical chemistry. 1998;44(7):1529-34.
49. Turroni F, Milani C, Duranti S, Mancabelli L, Mangifesta M, Viappiani A, et al. Deciphering bifidobacterial-mediated metabolic interactions and their impact on gut microbiota by a multi-omics approach. The ISME journal. 2016;10(7):1656-68.
50. Gosset G. Production of aromatic compounds in bacteria. Current opinion in biotechnology. 2009;20(6):651-8.
51. Mayneris-Perxachs J, Fernandez-Real JM. How the joint study of the microbiota and metabolites in different body fluids may aid in the identification of novel disease mechanisms. The FEBS journal. 2019.

52. Adam J, Brandmaier S, Leonhardt J, Scheerer MF, Mohney RP, Xu T, et al. Metformin Effect on Nontargeted Metabolite Profiles in Patients With Type 2 Diabetes and in Multiple Murine Tissues. Diabetes. 2016;65(12):3776-85.
53. Li X, Guo Y, Yan W, Snyder MP, Li X. Metformin Improves Diabetic Bone Health by Re-Balancing Catabolism and Nitrogen Disposal. PloS one. 2015;10(12):e0146152.
54. Kurilshikov A, van den Munckhof ICL, Chen L, Bonder MJ, Schraa K, Rutten JHW, et al. Gut Microbial Associations to Plasma Metabolites Linked to Cardiovascular Phenotypes and Risk. Circulation research. 2019;124(12):1808-20.
55. Lever M, George PM, Slow S, Bellamy D, Young JM, Ho M, et al. Betaine and Trimethylamine-N-Oxide as Predictors of Cardiovascular Outcomes Show Different Patterns in Diabetes Mellitus: An Observational Study. PloS one. 2014;9(12):e114969.
56. Murphy R, Tsai P, Jullig M, Liu A, Plank L, Booth M. Differential Changes in Gut Microbiota After Gastric Bypass and Sleeve Gastrectomy Bariatric Surgery Vary According to Diabetes Remission. Obesity surgery. 2017;27(4):917-25.

Tables

Table 1 Characteristics of the study cohort

	HC (N=55)	SCAD (N=71)	SCA+DM (N=38)	*P* value
Age, yrs*	55.56 ± 9.48	62.26 ± 8.91	63.53 ± 10.06	<0.001[bc]
Gender, n (M/F) §	27/28	49/22	27/11	0.035[bc]
BMI, kg/□*	24.09 ± 3.53	24.30 ± 2.83	27.08 ± 3.38	<0.001[ac]
SBP, mmHg†	120 (110, 125)	131 (118.5, 140)	133.5 (125.5, 148)	<0.001[bc]
Gensini score†	NA	31 (23, 51.75)	38.5 (27.75, 64.38)	0.298[a]
Current smoke§	8 (14.5%)	28 (39.4%)	14 (36.8%)	0.006[bc]
Medication				
Antihypertensive drugs§	0 (0)	45 (63.4%)	18 (47.4%)	<0.001[bc]
Statins§	0 (0)	48 (67.6%)	26 (68.4%)	<0.001[bc]
Oral hypoglycemic drug[s]	0 (0)	0 (0)	19 (50%)	<0.001[ab]
Insulin §	0 (0)	0 (0)	8 (21.1%)	<0.001[ab]
Laboratory data				
TG, mmol/L†	1.31 (0.92, 1.69)	1.20 (0.87, 1.80)	1.5 (1.16, 2.25)	0.125
TC, mmol/L†	4.49 (4.01, 5.32)	3.82 (3.23, 4.82)	3.81 (3.29, 4.40)	<0.001[bc]
LDL-C, mmol/L†	2.66 (2.23, 3.17)	2.23 (1.78, 2.78)	2.09 (1.7, 2.33)	<0.001[bc]
HDL-C, mmol/L†	1.1 (0.99, 1.33)	1.04 (0.81, 1.18)	0.92 (0.81, 1.14)	0.001[bc]
FBG, mmol/L†	6.2 (5.5, 7.95)	5.9 (5.2, 6.9)	8.75 (7.4, 12.3)	<0.001[ab]
HbA1c, %†	NA	5.6 (5.2, 6.6)	6.75 (5.5, 7.4)	0.001[a]
HOMA IR†	3.93 (2.81, 5.34)	3.97 (3.35, 5.16)	8.18 (5.17, 10.16)	<0.001[ab]
HOMA β†	113.88 (67.15, 151.76)	125.64 (84.49, 164.34)	72.17 (41.03, 112.99)	0.017[ab]
CK, U/L†	119 (97.5, 134)	88 (65.5, 121.5)	111.5 (77.25, 161.25)	0.001[ac]
CK-MB, U/L†	0.8 (0.5, 1.05)	0.7 (0.5, 1)	1 (0.6, 1.5)	0.032[a]
cTnI, ug/L†	0 (0, 0)	0 (0, 0.01)	0.01 (0, 0.03)	<0.001[abc]
hs-CRP, mg/L†	0.71 (0.39, 1.25)	1.06 (0.57, 2.13)	1.21 (0.50, 2.66)	0.113

†median (IQR), *mean ± SD, §n (%), NA not available.

Continuous, normally distributed variables among the four groups were analysed by a one-way analysis of variance. The Kruskal-Wallis H-test was applied for data of this type that were not normally distributed. Continuous, normally distributed variables between two groups were analysed by Student's t-test. The Mann- Whitney U test was applied for data of this type that were not normally distributed. Categorical variables were compared by the $\chi 2$ test. [a]$P < 0.05$ for equality between SCAD+DM vs. SCAD. [b]$P < 0.05$ for equality between SCAD+DM vs. HC. [c]$P < 0.05$ for equality between SCAD vs. HC.

Table 2 Cohort characteristics of major cardiovascular incidence and mortality

Outcome	SCAD (n=71) No. of event/total	SCAD+DM (n=38) No. of event/total	P Value
Primary endpoint	1/1.41%	3/7.89%	0.0861
Secondary endpoint			
Hospitalization	13/18.31%	8/21.05%	0.7293
Procedures	5/7.04%	2/5.26%	0.7181

The primary endpoint was the time to the first major cardiovascular event including all-cause death, nonfatal myocardial infarction and stroke. Secondary endpoints were any coronary heart disease event including unstable angina, arrhythmia and congestive heart failure requiring hospitalization or an ischemia-driven coronary revascularization procedure such as invasive coronary angiography, percutaneous transluminal coronary intervention and coronary artery bypass graft.

Figures

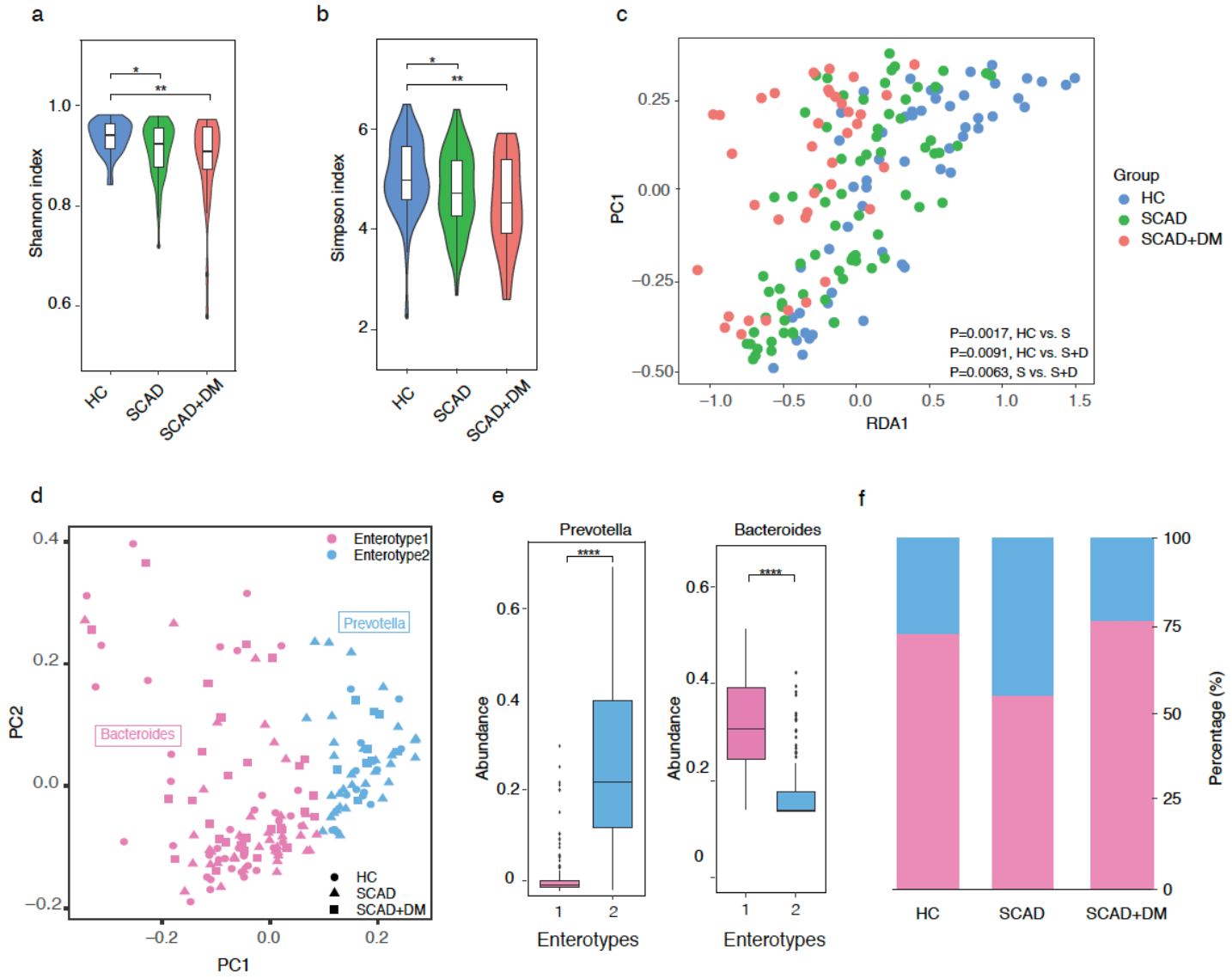

Figure 1

Gut microbial characteristics of the gut microbiome in study subjects with SCAD and SCAD+DM. a,b) α-diversity analysis showing that SCAD and SCAD+DM patients were characterized by lower microbial richness in Shannon and Simpson indexes based on genera profiles relative to healthy controls (n = 55, HC; n = 71, SCAD; n = 38, SCAD+DM). c) Differentially changed genera in SCAD, SCAD+DM. and HC according to dbRDA based on Bray–Curtis distance. d) A total of 164 samples are clustered into enterotype 1 (pink) and enterotype 2 (blue) by PCoA of Jensen-Shannon divergence values at the genus level. The major contributor in the two enterotypes is Bacteroides and Prevotella, respectively. e) Relative abundances of the top genera (Bacteroides and Prevotella) in each enterotype. $P < 0.0001$ and $P < 0.0001$, respectively; Wilcoxon rank sum test. f) The percentage of HC, SCAD and SCAD+DM samples distributed in two enterotypes. Boxes represent the inter quartile ranges, the inside line or points represent the median, and circles are outliers

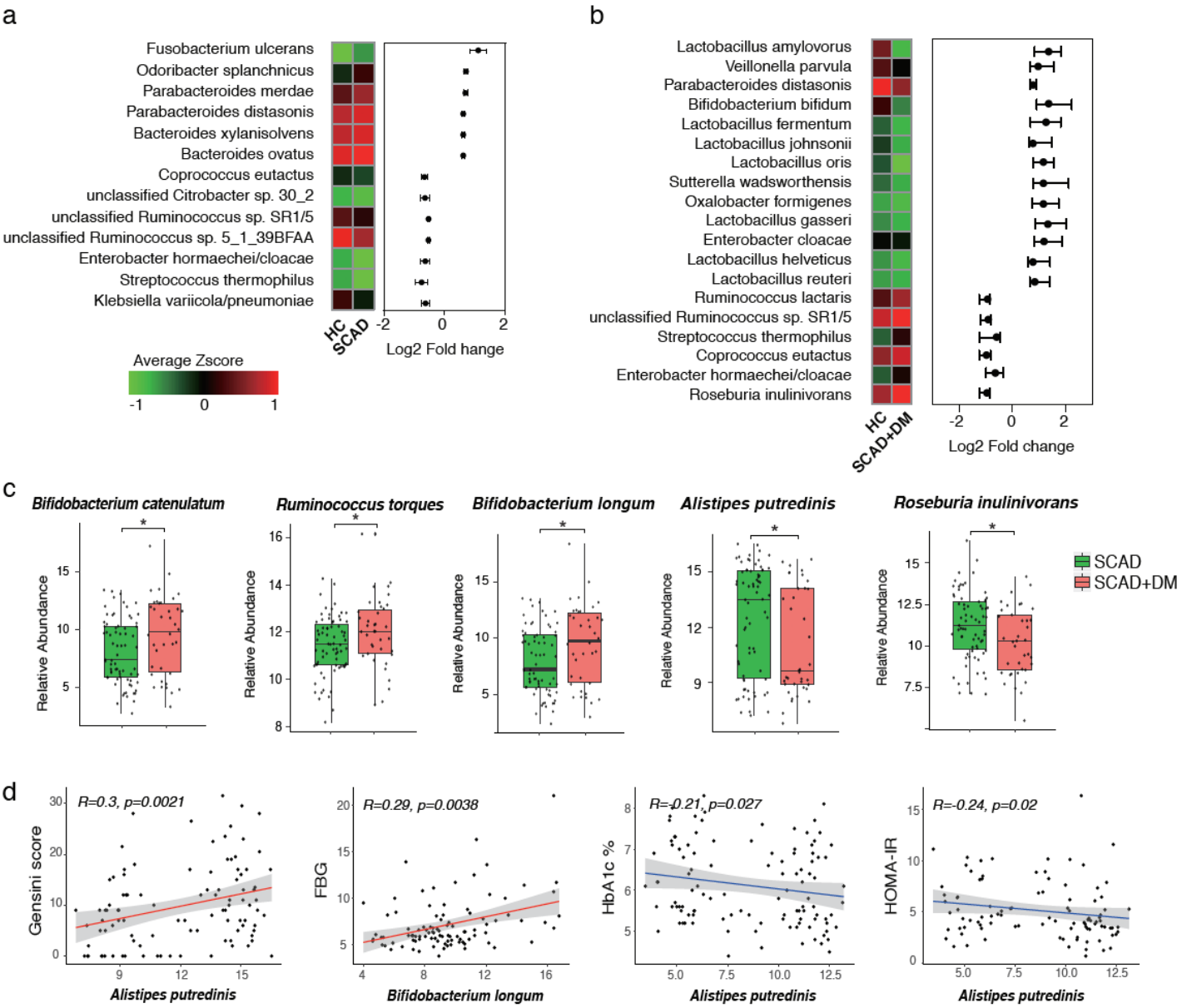

Figure 3

Gut microbial species varied across different groups. a) Heatmap showing the relative fold change of species in SCAD group against HC group. b) Heatmap showing the relative fold change of species in SCAD+DM group against HC group. In a) and b), the abundance profiles were transformed into Z scores by subtracting the average abundances and dividing the standard deviations of all the samples. Species with absolute log2 fold change greater than 0.5 and P value < 0.05 were selected as metagenomics candidates. c) Species significantly changed in SCAD+DM group compared with SCAD group. P value < 0.05, Wilcoxon test. d) Spearman correlation between significantly varied species and atherosclerotic severity indicator and major diabetic phenotype.

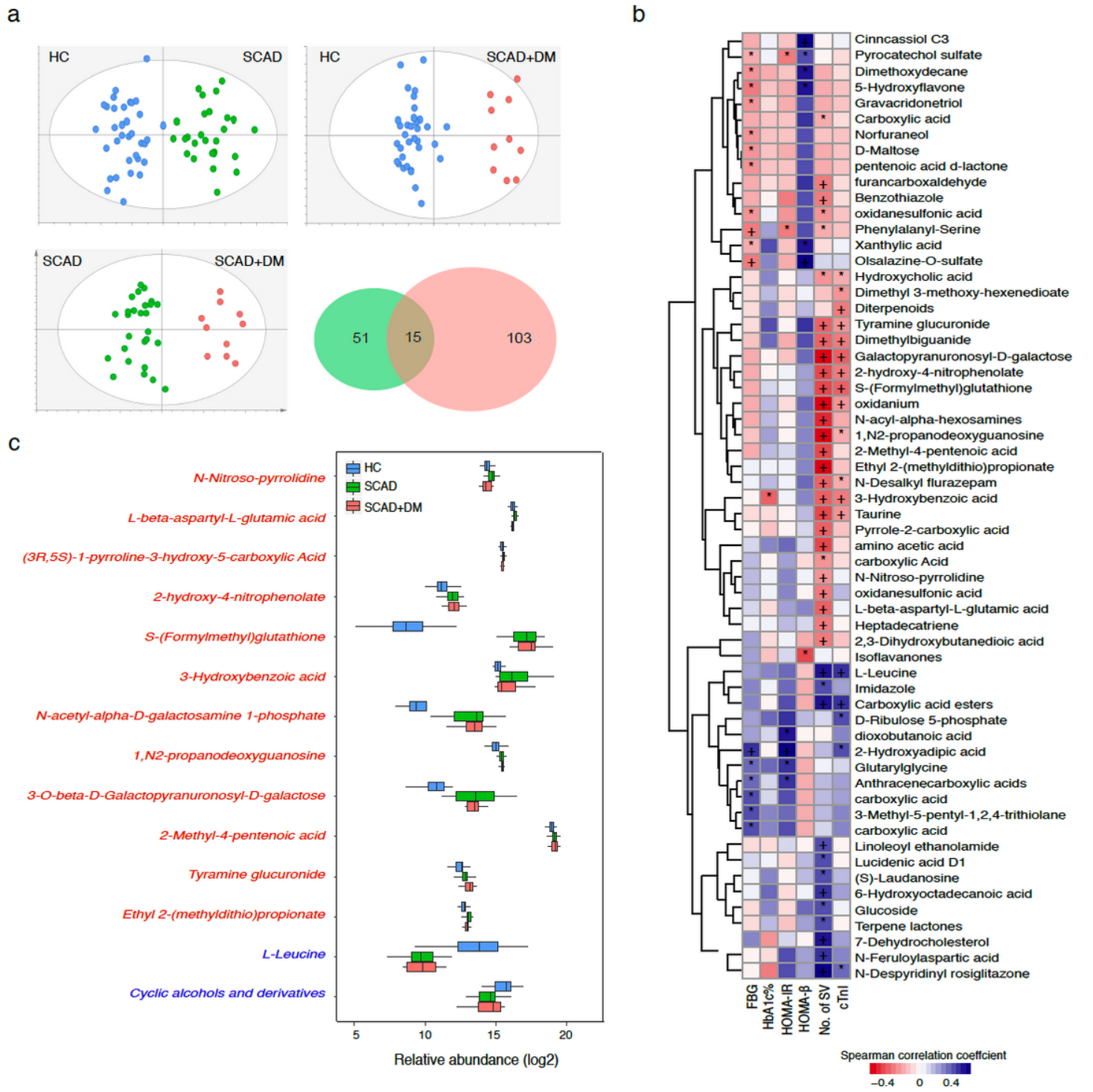

Figure 5

Aberrant metabolic patterns in SCAD and SCAD+DM groups. a) Score scatter plots of OPLS-DA comparing the serum metabolic differences identify the separation between HC vs. SCAD, HC vs. SCAD+DM, and SCAD vs. SCAD+DM, respectively. Metabolites significantly changed in SCAD or SCAD+DM as compared to control at VIP >1 and adjusted P value < 0.05 are identified. Venn diagrams demonstrate the number of altered metabolites shared between SCAD (green) and SCAD+DM (red) by the overlap. b) Spearman correlations between serum metabolites and major diabetic and atherosclerotic

phenotypes. The color represents positive (red) or negative (blue) correlations, and FDRs are denoted as follows: *FDR < 0.05, +FDR < 0.01. c) The box plot shows that the serum metabolites significantly changed between different groups according to the Wilcoxon rank sum test. The names of the metabolites comprising the AS+ and AS-metabotypes are highlighted in red and blue, respectively.

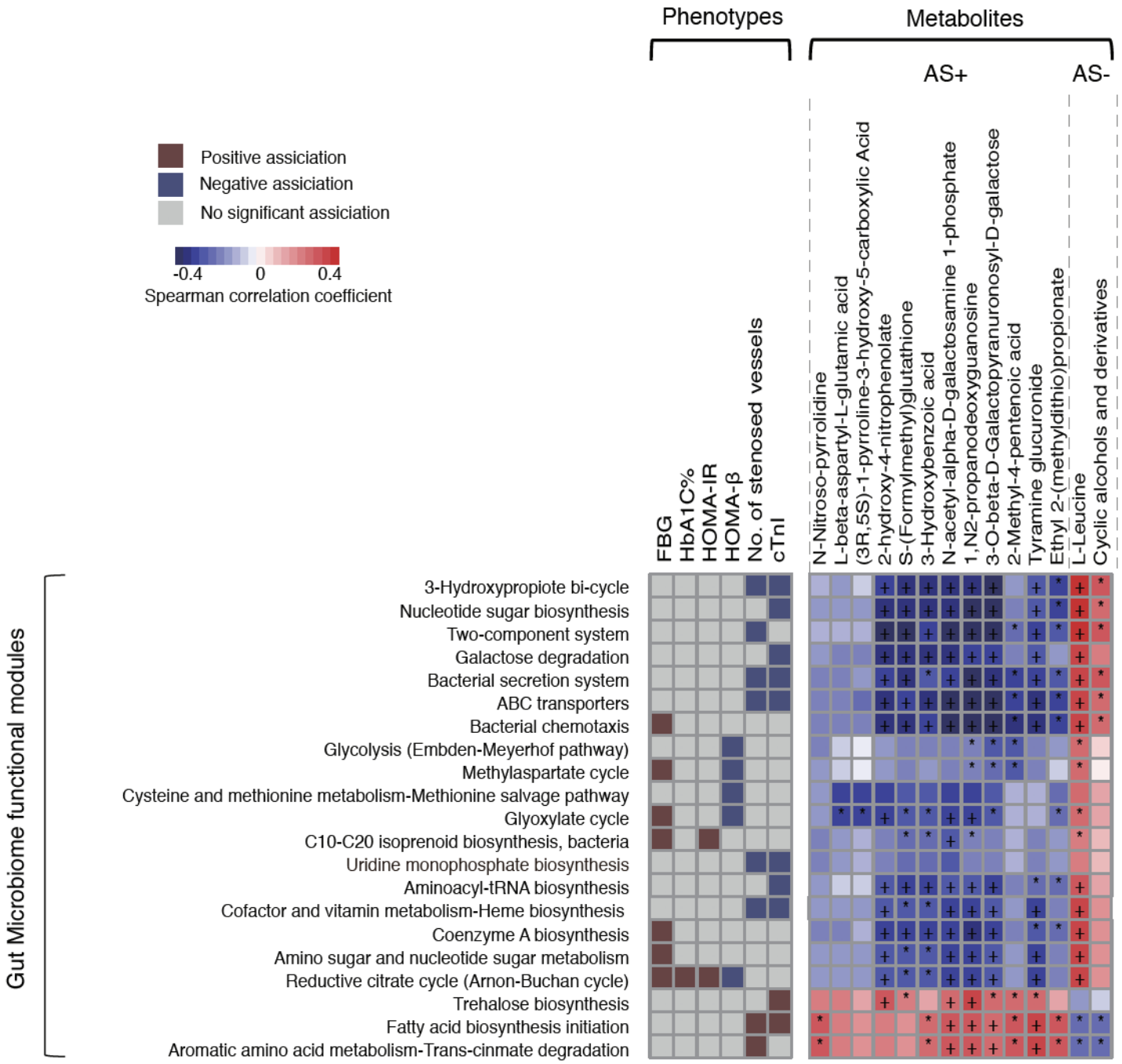

Figure 7

Association map of the three-tiered analyses integrating the phenome, the gut microbiome, and the fasting serum metabolome in study cohorts. The left panel shows significant associations (Mann–Whitney U-test; FDR < 0.05) between microbial functional modules and the indicated phenotypes; coloring indicates direction of association. The right panel shows associations between the same bacterial

modules and serum metabolite clusters. Coloring represents the median Spearman correlation coefficient between metabolite clusters and the indicated functional modules, where FDRs are denoted: *, FDR < 0.05; +, FDR < 0.01.

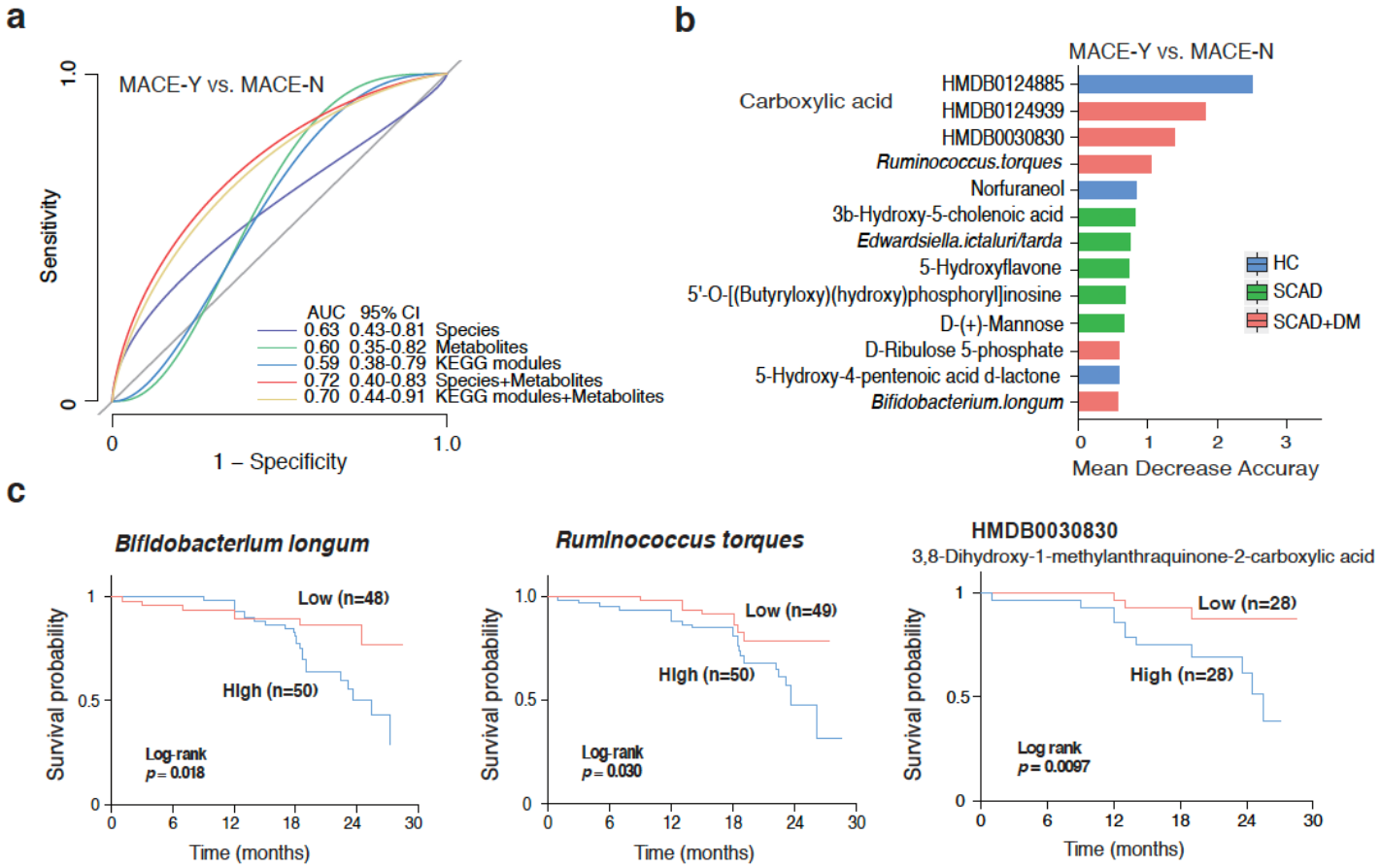

Figure 9

Potential of species and metabolites for cardiovascular disease prognosis. a) Random forest models are constructed using explanatory variables of species, metabolites, species + metabolites, KEGG modules + metabolites. The AUC shows the classification of major adverse cardiac event during follow-up. The species + metabolites based classification is more efficient as indicated by a higher AUC. b) The detailed explanatory variables based on the species + metabolites comparison. The lengths of the bars in the histogram represent the mean decrease accuracy, which indicates the importance of features for prediction. c) Kaplan-Meier estimates for survival probability based on the abundance levels of predictive variables.

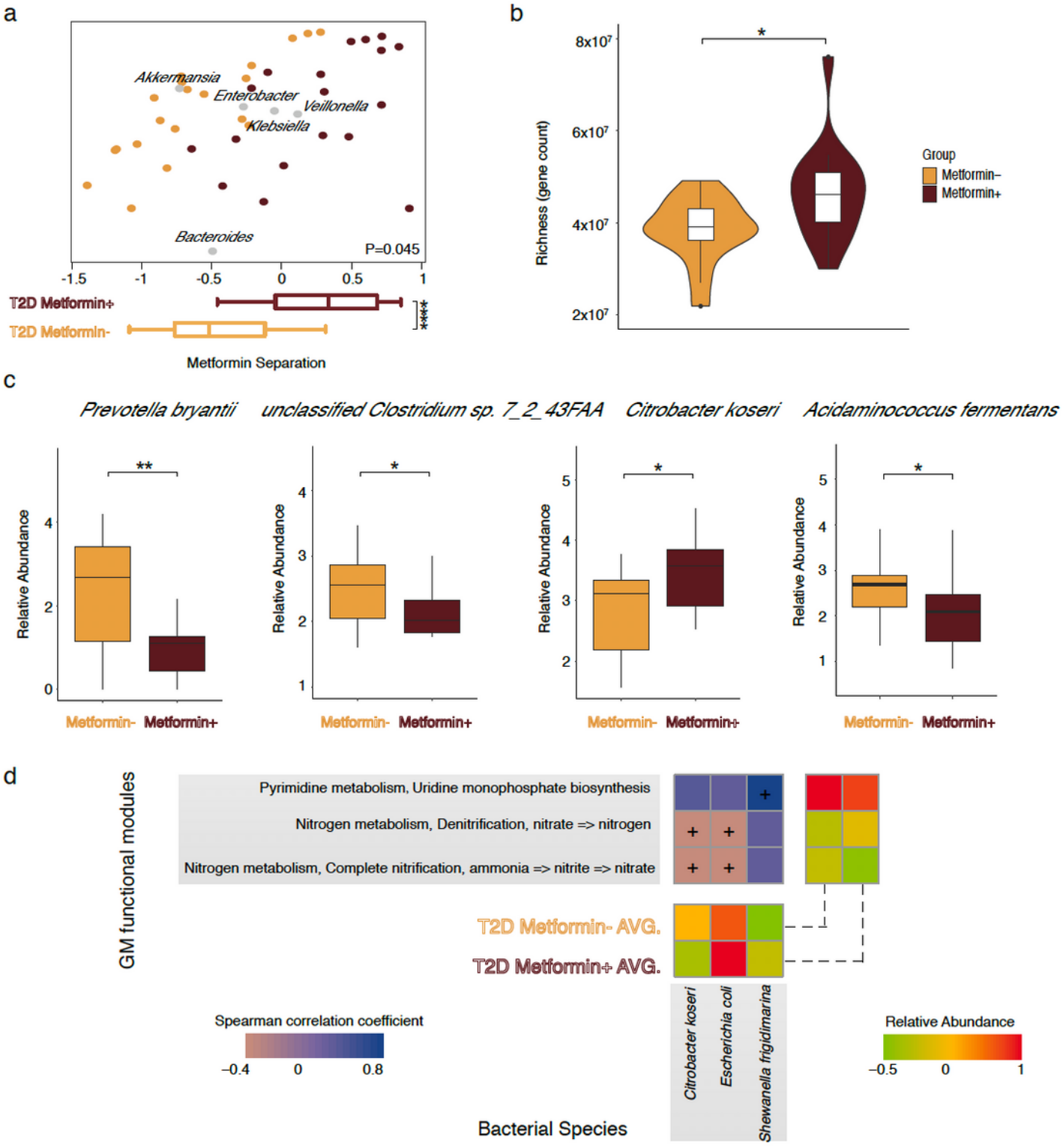

Figure 11

T2DM gut microbiome is confounded by metformin treatment. a) Projection of genus-level gut microbiome samples constrained by metformin treatment. Bacterial genera that show significant effects of metformin treatment (limited to top five), are interpolated into the plane of maximal separation based on their abundances across all samples. Marginal box plots show the separation of the constrained projection coordinates, the metformin separation is significant. b) Elevated gene richness in SCAD+DM

samples. Compared with Metformin-untreated samples, Metformin-treated gut metagenomes show significantly higher gut microbiome richness (Mann–Whitney U-test). Sample median richness is shown as horizontal black bars. c) Gut microbial shifts under metformin treatment (P value < 0.05, Wilcoxon test). Boxes represent the inter-quartile ranges, and lines inside the boxes denote medians. d) The heat maps show bacterial species (horizontal axis) and microbial gene functions (vertical axis) that are significantly different in abundance (enrichment scores shown as intensity of innermost marginal heat maps; red–green color scale) between T2DM metformin-treated and metformin-untreated gut metagenomes. The central heat map shows Spearman correlations (purple–red color scale) between abundance of bacterial taxa and microbial gene modules (Spearman test FDR scores: * FDR < 0.05, + FDR < 0.01).

Supplementary Files

This is a list of supplementary files associated with this preprint. Click to download.

- Additionalfile2.pdf
- Additionalfile1.xlsx
- Additionalfile1.xlsx
- Additionalfile2.pdf